

# Unconventional Gross-Neveu quantum criticality: interaction-induced SO(3)-biadjoint insulator and emergent SU(3) symmetry

Shouryya Ray\*

CP3-Origins, University of Southern Denmark, Campusvej 55, DK-5230 Odense M, Denmark

(Dated: June 28, 2024)

I point out that Gross-Neveu theory with SO(3) isospin in three spacetime dimensions—proposed recently, for instance, as an effective description of the Néel transition in certain spin-orbital liquids—also hosts quantum criticality of a more exotic kind. The ordered phase breaks SO(3) spontaneously, but the SO(3)-Néel order parameter vanishes. The fermionic bilinear order parameter is instead a biadjoint with respect to SO(3); unlike its Néel cousin, it constitutes an interaction-induced insulator. Furthermore, I show that the Néel and biadjoint order parameters can be combined to transform as an adjoint under SU(3) symmetry; the symmetry is emergent at the critical point separating the symmetric semimetal and the biadjoint insulator, but only if the flavor number is small enough, suggesting order-parameter fluctuations and the interplay between different channels play a crucial role in stabilizing the enlarged symmetry. In candidate SO(3) spin-orbital liquids, thermodynamic critical exponents carry fingerprints of “spinons”. The existence of an independent universality class in addition to the Néel transition opens the possibility of posing further constraints on spinon properties from thermodynamic measurements near criticality alone.

## I. INTRODUCTION

Quantum critical phenomena beyond the Ginzburg-Landau paradigm are a cornerstone of the modern theory of quantum phase transitions.<sup>1</sup> Commonly, this entails degrees of freedom beyond order-parameter excitations that become soft at criticality; in a Fermi system, this role is played by fermionic degrees of freedom that “live” on the Fermi surface. In  $d > 1$  spatial dimensions, the Fermi surface generically has co-dimension one, leading to an uncountable infinitude of such modes and an effective theory that is usually intractable analytically.<sup>2</sup> The situation improves drastically in *Dirac semimetals*, where the Fermi surface consists of isolated points in reciprocal space and the fermions disperse linearly close to the Fermi points, leading to emergent Lorentz symmetry near criticality. Quantum phase transitions in such materials are described by Gross-Neveu theory in  $D := d + 1$  spacetime dimensions (GN<sub>D</sub> for short); I shall mainly focus on quasi-planar materials—for which graphene is arguably the most celebrated exponent<sup>3</sup>—so  $D = 3$  unless stated otherwise. However, boiling down the effectiveness of GN<sub>3</sub> theory to its applicability in Dirac semimetals, or even statistical physics short-changes it somewhat. Among other things, GN<sub>3</sub> (more generally, GN<sub>2<D<4</sub>) constitutes a particularly simple, and thereby tractable, example of *asymptotic safety* [21], which is a highly predictive candidate for the UV completion of the Standard Model coupled to Einstein-Hilbert gravity.<sup>4</sup> Therein, quantum fluctuations of the spacetime metric tensor are supposed to offset the clas-

sical breaking of scale symmetry through dimensionful couplings such as the Newton coupling, in analogy with how quantum fluctuations enable the perturbatively non-renormalizable Fermi coupling to reach scale invariance in GN<sub>3</sub>. Since gravity fluctuations only become strong at planckian scales inaccessible to current accelerators, quantum criticality of the GN<sub>3</sub> family is at the moment perhaps the only example of asymptotic safety with fermionic matter that can be observed in the laboratory.

A significant recent application of Gross-Neveu quantum criticality is furnished by a class of novel phases of matter called spin-orbital liquids. In many regards, they behave like a Dirac semimetal, albeit one made of *spinons*—fermionic quasiparticles arising due to fractionalization of the electron’s spin-orbital moment—rather than elementary electrons (as would be the case in graphene) themselves. It is impossible to excite spinons in a coherent fashion: an experimentally feasible protocol like flipping a magnetic moment excites a continuum of spinons. What is comparatively feasible is to destabilize a spin-orbital liquid in favor of a conventionally ordered phase and detect the onset of said order. The exponents which describe the non-analyticity of thermodynamic observables close to criticality—called thermodynamic critical exponents—still carry “fingerprints” of the spinons. This makes the study of quantum criticality of the GN<sub>3</sub> family a promising component of the toolkit towards the diagnostic of novel phases of matter (in addition to all the afore-mentioned merits of GN<sub>2<D<4</sub>). It has been proposed [25] that a potential quantum phase transition to Néel order in a candidate SO(3) spin-orbital liquid (e.g., in spin-orbit coupled double perovskites like Ba<sub>2</sub>YMoO<sub>6</sub> [26, 27]), would be describable using GN<sub>3</sub> theory with SO(3) isospin [GN<sub>3</sub>-SO(3) theory for short]; onset of Néel order would then correspond to spontaneous symmetry breaking (SSB) of the SO(3) isospin symmetry by the condensation of the fermion bilinear  $\bar{\psi} L_a \psi$ , with  $L_a$  ( $a = 1, 2, 3$ ) the generators of SO(3) in the fundamental representation. A more thorough understanding of GN<sub>3</sub>-SO(3) quantum criticality is hence worth pursuing.

GN<sub>3</sub>-SO(3) does have a more prominent cousin, GN<sub>3</sub>-

\* sray@cp3.sdu.dk

<sup>1</sup> See, for instance, textbooks such as [1–3]

<sup>2</sup> Notable exceptions where some controlled analytical progress has been possible include [4–9]; see also [10] for attempts to go beyond perturbation theory.

<sup>3</sup> cf., e.g., [11–18]; an example where the “semimetal” is formed due to  $d$ -wave superconductivity in a metal is discussed in [19]; for a recent review of quantum criticality in Dirac semimetals, cf. [20].

<sup>4</sup> See [22] for a pedagogical introduction and [23, 24] for reviews on the current state of the art.

SU(2), which has been studied more extensively since it concerns graphene’s putative antiferromagnetic quantum critical point [28–31]. A significant difference between SO(3) and SU(2) is that SO(3) generators have a zero eigenvalue: when  $\bar{\psi}L_a\psi$  condenses, the effective mass matrix of the fermions inherits this zero eigenvalue. The SO(3)-Néel transition is hence a semimetal-to-semimetal transition, dubbed “metallic” quantum criticality. By contrast, SU(2) generators have no vanishing eigenvalue, and the Néel-ordered phase is an interaction-induced (also called Mott) insulator.<sup>5</sup>

In this Article, I shall focus on a further peculiarity of GN<sub>3</sub>-SO(3): unlike SU(2) [or for that matter any SU( $N_{\text{iso}}$ )], it is possible to break SO(3) isospin symmetry in Lorentz-invariant fashion at the level of fermion bilinears without giving the Néel bilinear  $\bar{\psi}L_a\psi$ —which transforms as a vector<sup>6</sup> under SO(3)—a vacuum expectation value (vev). The resulting phase instead sees a different bilinear obtain a vev. This bilinear transforms as a *biadjoint*<sup>7</sup> under SO(3) and gaps out the fermion spectrum entirely: it is an interaction-induced insulator phase. My main findings can then be summarized as in Fig. 1, in terms of phase diagrams as a function of density-density (aka 4-Fermi) couplings  $g_{01}$  and  $g_{02}$  associated at mean-field level with the Néel and biadjoint order parameters respectively [see Eq. (4) for a more precise definition]. For large enough flavor number, an effectively single-channel description is valid. The transition to the interaction-induced SO(3)-biadjoint insulator [SO(3)<sub>2</sub> for short] is governed by a distinct critical fixed point, as is the Néel [= SO(3)<sub>1</sub>] transition. The SO(3)<sub>1</sub> and SO(3)<sub>2</sub> order parameters can be formally combined to form an adjoint under SU(3) for appropriate couplings, but the corresponding fixed point is then bicritical: SU(3) symmetry is unstable. This changes at small flavor number. In this regime, non-trivial interplay between fluctuations of different order parameters stabilizes SU(3) symmetry. As a consequence, the GN-SO(3)<sub>2</sub> fixed point becomes unstable, and the SO(3)<sub>2</sub> transition is governed by the GN-SU(3) fixed point instead. The interaction-induced SU(3) and SO(3)<sub>2</sub> insulators feature the same fermionic single-particle spectrum, but there are robust qualitative differences,

such as in the number of Nambu–Goldstone bosons (NGBs); in addition, the SO(3)<sub>1</sub> susceptibility diverges with the same power law as the SO(3)<sub>2</sub> one at criticality due to the enlarged symmetry.

The calculations supporting these conclusions will be performed using renormalization group (RG) at one-loop. I provide the RG flow equations (“beta functions”) for all SO(3)-compatible 4-Fermi interactions, a Fierz-complete basis for which I have constructed. This is a technical challenge of independent interest, and already relevant to the conventional Néel channel<sup>8</sup> ( $\bar{\psi}L_a\psi$ )<sup>2</sup> studied before in [25, 32], because it is not closed under renormalization; the only non-abelian isospin GN theory for which Fierz-complete beta functions have been computed is GN<sub>2</sub>-SU(2) [33]. The present one should hence be a welcome addition to this rather sparse “stamp collection”.

## II. THEORY SPACE OF GN<sub>3</sub>-SO(3)

To derive RG flow equations, we first need to write down a Gross-Neveu-like action which we can be sure will remain closed under renormalization. To do so amounts to writing down all 4-Fermi operators compatible with SO(3) symmetry. The Lie algebra of SO(3) is characterized by its structure constants,  $[L_a, L_b] = i\varepsilon_{abc}L_c$ , where  $\varepsilon_{abc}$  is the Levi-Civita symbol. In the fundamental representation, the  $L_a$  act on a three-dimensional vector space. Along with the identity  $\mathbb{1}_3$  (usually not written out in products), the SO(3) generators thus provide only 4 elements; the space of 3-dimensional matrices has dimension 9. The five missing matrices may be taken to be  $Q_{ab}$ , the independent components of the traceless symmetric combination

$$Q_{ab} = \{L_a, L_b\}/2 - (2/3)\delta_{ab} \quad (1)$$

where  $\{\cdot, \cdot\}$  denotes the anti-commutator. The  $Q_{ab}$ ’s commutation relation with the  $L_a$  reads

$$[L_a, Q_{bc}] = i(\varepsilon_{abd}Q_{dc} + \varepsilon_{acd}Q_{bd}). \quad (2)$$

Consider now an infinitesimal isospin rotation  $\delta_{\epsilon_a}\psi = i\epsilon_a L_a\psi$  (and h.c. for  $\bar{\psi} := \psi^\dagger\gamma_0$ ). Under such a transformation, a fermion bilinear transforms as

$$\delta_{\epsilon_a}(\bar{\psi}O\psi) = i\epsilon_a(\bar{\psi}[L_a, O]\psi). \quad (3)$$

In other words, the generators of SO(3) act on fermion bilinears in adjoint fashion;  $\bar{\psi}L_a\psi$  transforms as an *adjoint* under SO(3) and  $\bar{\psi}Q_{ab}\psi$  as a *biadjoint*. The above commutation relations further mean both  $(\bar{\psi}L_a\psi)^2$  and  $(\bar{\psi}Q_{ab}\psi)^2$  are invariant under SO(3) rotations. Tensoring  $\mathbb{1}_3$ ,  $L_a$  and  $Q_{ab}$  with Lorentz-covariant quantities leads to<sup>9</sup>

$$\mathcal{L}_{\text{GN}_3\text{-SO}(3)} = \bar{\psi}_i\delta\psi_i - \frac{g_{00}}{2N_f}(\bar{\psi}_i\psi_i)^2 - \frac{g_{10}}{2N_f}(\bar{\psi}_i\gamma_\mu\psi_i)^2$$

<sup>5</sup> The terminology semimetal vis-a-vis interaction-induced/Mott insulator is used somewhat liberally here. In the strict sense of those words, they refer to the presence or absence of electrically charged quasiparticles at the Fermi level. Charge here in turn refers to the physical charge of the electron, i.e., the property of being charged under the U(1) gauge symmetry associated with the photon. In that stricter sense, an SO(3) spin-orbital liquid is already a Mott insulator, because spinons do not carry a U(1) electric charge. For the purposes of this Article, however, any and all fermionic excitations will count towards a Fermi surface, regardless of whether these fermions have any overlap with single-particle electron states. By this logic, a state is an interaction-induced (i.e., a Mott) insulator only if it has an interaction-induced gap at the Fermi level with respect to all fermionic quasiparticles. In the remainder, the qualifiers interaction-induced and Mott are furthermore taken to be synonymous and dropped for the sake of brevity when clear from context.

<sup>6</sup> We shall in fact see below that it is more precisely an adjoint vector, though for SO(3) the two notions are ultimately equivalent.

<sup>7</sup> Again, as discussed in more detail later, the “biadjoint” is equivalent to “symmetric traceless rank-2 tensor” for SO(3). If one likes to think of the bilinear  $\bar{\psi}L_a\psi$  as a dipole moment in isospin space, then the biadjoint bilinear is, in the same vein, conducive to interpretation as a *quadrupole* moment in isospin space.

<sup>8</sup> This is true for the Néel channel corresponding to any non-abelian isospin symmetry.

<sup>9</sup> Throughout, I shall work in Euclidean signature;  $\delta := \gamma_\mu\partial_\mu$

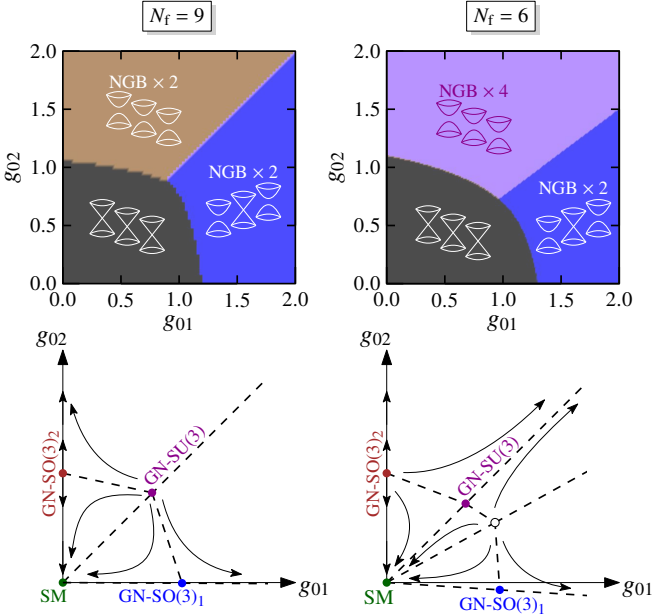


FIG. 1. Top row: Phase diagrams as function of 4-Fermi couplings [see Eq. (4) for definitions] for interaction-induced transitions from symmetric semimetal (SM) to Lorentz invariant SO(3) isospin-broken phases in three-dimensional Gross-Neveu theory; insets show the fermions’ single-particle spectrum, along with the number of Nambu-Goldstone bosons (NGBs) where applicable. Bottom row: Corresponding RG phase portraits, with fixed points [projected to the  $(g_{01}, g_{02})$  plane] denoted by solid circles and (projections of) RG-invariant subspaces denoted by heavy dashed lines; flow lines are schematic and not to scale. Left:  $N_f = 9$ . In this regime, the mean-field picture is qualitatively valid. In addition to the usual Néel [ $:= \text{SO}(3)_1$ ] transition, there is a transition to an SO(3)-biadjoint insulator [ $:= \text{SO}(3)_2$ ] governed by the finite- $N_f$  descendant of the large- $N_f$  fixed point; the SU(3) symmetric subspace is IR-unstable. Right:  $N_f = 6$ . While the stability of SO(3)<sub>1</sub> remains unchanged, SU(3) symmetry emerges for  $N_f < N_{f,\text{cr}} \approx 6.5$  in the IR at a putative GN-SO(3)<sub>2</sub> transition. The fermions’ single-particle spectrum is qualitatively the same, but robust qualitative differences in the SO(3)<sub>2</sub> vis-a-vis SU(3) scenarios include a distinct number of NGBs. There is a bicritical fixed point (white) not adiabatically connected to any mean-field limit; for  $9 < N_f < 6$ , it collides first with GN-SO(3)<sub>2</sub> and then GN-SU(3), realizing thus a transfer of stability between the two fixed points, before settling down between GN-SU(3) and GN-SO(3)<sub>1</sub> to form the phase boundary between the SO(3)<sub>1</sub> and SU(3) phases.

$$\begin{aligned}
 & -\frac{g_{01}}{8N_f}(\bar{\psi}_i L_a \psi_i)^2 - \frac{g_{11}}{8N_f}(\bar{\psi}_i \gamma_\mu L_a \psi_i)^2 \\
 & -\frac{g_{02}}{2N_f}(\bar{\psi}_i Q_{ab} \psi_i)^2 - \frac{g_{12}}{2N_f}(\bar{\psi}_i \gamma_\mu Q_{ab} \psi_i)^2. \quad (4)
 \end{aligned}$$

Two remarks are in order. (i) the Clifford algebra  $\{\gamma_\mu, \gamma_\nu\} = 2\delta_{\mu\nu}\mathbb{1}_{d_\gamma}$  is meant to be taken in its irreducible representation. In  $D = 3$ , this means  $d_\gamma = 2$ . This in turn means the matrices  $[\gamma_\mu, \gamma_\nu]$  which generate the spinorial part of Lorentz transformations are  $\sim \varepsilon_{\mu\nu\rho}\gamma_\rho$  and do not furnish independent channels. Furthermore, the odd spacetime dimension and the irreducibility of the representation as usual combine to make  $\gamma_5 = i\gamma_0\gamma_1\gamma_2 \sim \mathbb{1}_2$ . (ii) I have instated a flavor index

$i = 1, \dots, N_f/3$  with  $N_f \in 3\mathbb{N}_{>0}$  in physical cases (in other words,  $N_f$  counts the number of two-component fermions). It is distinct from the isospin index: the flavor structure is untouched by isospin rotations, and the theory as a whole is to be symmetric under flavor rotations. Eq. (4) contains only the flavor-singlet combinations; flavor non-singlet 4-Fermi operators are not generated, and can in any case be re-written as a linear combination of flavor-singlet ones using Fierz identities.

The subspace within the GN<sub>3</sub>-SO(3) theory space satisfying  $g_{r1} = g_{r2}$  for  $r = 0, 1$  features an enhanced symmetry, viz., SU(3). This may be made manifest by gathering the  $(L_a)$  and  $(Q_{ab})$  together into one set as

$$(\Lambda_\alpha) = (L_a/2, Q_A) \quad (5)$$

with

$$(Q_A) = \left( Q_{23}, Q_{13}, Q_{12}, \frac{1}{2}(Q_{11} - Q_{22}), \frac{\sqrt{3}}{2}Q_{33} \right). \quad (6)$$

The suggestive notation is to be taken seriously: the  $\Lambda_\alpha$  obey  $\text{Tr}(\Lambda_\alpha \Lambda_\beta) = \delta_{\alpha\beta}/2$  and  $[\Lambda_\alpha, \Lambda_\beta] = if_{\alpha\beta\gamma}\Lambda_\gamma$ , where  $f_{\alpha\beta\gamma}$  are the SU(3) structure constants. (Most economically, this is seen by noticing that, up to a renumbering of  $\alpha$ , the  $\Lambda_\alpha$  are proportional to the Gell-Mann matrices.) The  $(\Lambda_\alpha)$  are hence a bona fide representation of SU(3)’s Lie algebra, in agreement with results on the SU(3)  $\supset$  SO(3) “missing label” problem in representation theory.<sup>10</sup>

### III. THE INTERACTION-INDUCED BIADJOINT INSULATOR

Before proceeding to the renormalization of GN<sub>3</sub>-SO(3), let us pause to consider the non-Néel isospin-broken phase characterized by  $\langle \bar{\psi} L_a \psi \rangle = 0$ ,  $\langle \bar{\psi} Q_A \psi \rangle \neq 0$ . (I shall focus only on Lorentz-invariant phases henceforth.) In the limit  $N_f \rightarrow \infty$ , mean-field theory becomes exact, and the effective potential for the order parameter (OP)  $\phi_A = \bar{\psi} Q_A \psi$  near  $\phi_A = 0$  reads

$$\begin{aligned}
 V_{\text{eff}}(\phi_A) &= \frac{|\phi_A|^2}{2g_{02}} - \text{Tr} \ln (\not{\partial} + \phi_A Q_A) \\
 &= V_{\text{eff}}(0) + \frac{|\phi_A|^2}{2g_{02}} + \sum_{\sigma=1}^3 \left( -\frac{M_\sigma^2}{2\pi^2} + \frac{|M_\sigma|^3}{6\pi} \right) + \mathcal{O}(\phi_A^4). \quad (8)
 \end{aligned}$$

Some comments regarding the evaluation of the “trace-log” formula in Eq. (7) are in order. The operator trace Tr contains both an integration over all momenta as well as a trace over spinor, isospin and flavor indices. The flavor trace yields an overall factor  $N_f$ , which has been absorbed into the definition

<sup>10</sup> In the mathematical literature, the inverse problem of labelling representations of SU(3) by representations of its subalgebra is called the “missing label” problem, on which there is a quite extensive body of research. A classical review is [34].

of the effective potential,  $V_{\text{eff}} \rightarrow V_{\text{eff}}/N$ . The trace over spinor and isospin indices begets a sum over all eigenvalues of the effective mass matrix,  $(M_\sigma) := \text{eigs}(\phi_A Q_A)$ . To compute these eigenvalues, let us work in the *defining* representation,<sup>11</sup> where the generators have components

$$(L_a)_{ij} = i\epsilon_{aij}. \quad (9)$$

Then,  $Q_4 \sim \text{diag}(1, -1, 0)$  and  $Q_5 \sim \text{diag}(-1, -1, 2)$  are represented by real, diagonal matrices. The mass matrix  $\phi_A Q_A$ , on the other hand, is hermitean and traceless [being in fact an element of  $\text{SU}(3)$ 's Lie algebra, essentially due to the observation in Eqs. (5)–(6) above]. Consequently, it can be diagonalized, and furthermore be written as a linear combination of the matrices representing  $Q_4$  and  $Q_5$ . In other words, one may choose, w.l.o.g., a frame where

$$\phi_A Q_A = \frac{1}{2} \text{diag} \left( \phi_4 - \frac{1}{\sqrt{3}}\phi_5, -\phi_4 - \frac{1}{\sqrt{3}}\phi_5, \frac{2}{\sqrt{3}}\phi_5 \right). \quad (10)$$

The integration over momenta is UV-divergent and needs to be cut off at some  $p^2 = k_{\text{UV}}^2$ . The  $k_{\text{UV}}$ -dependence can, however, be absorbed by measuring all dimensionful quantities in units of (suitable powers of)  $k_{\text{UV}}$ , i.e.,  $\phi_A \rightarrow \phi_A/k_{\text{UV}}$ ,  $V_{\text{eff}} \rightarrow V_{\text{eff}}/k_{\text{UV}}^3$  and  $g_{02} \rightarrow g_{02}k_{\text{UV}}$ .

A plot of the effective potential in the frame defined by Eq. (10) is shown in Fig. 2 in the symmetric vis-a-vis SSB phase. One finds that  $V_{\text{eff}}(\phi_A)$  is minimized for  $\phi_4 = 0$ ,  $|\phi_5| \propto |g - g_{\text{cr}}|$  if  $g_{02} > g_{\text{cr}} = \pi^2/2$ . The fact that the vev points in the  $A = 5$  direction is intuitive, since  $Q_5 \equiv \Lambda_8$  is the only mass matrix that has no zero eigenvalue. Strictly speaking, the statement is true only modulo  $(\phi_4 + i\phi_5) \rightarrow e^{i\frac{\pi}{3}n}(\phi_4 + i\phi_5)$  for  $n \in \mathbb{Z}$ . The corresponding operation on  $(Q_4, Q_5)$  sends  $Q_5$  to one that is unitarily equivalent (i.e., has the same eigenvalues), so I shall set  $n = 0$  w.l.o.g. Consequently, the fermions' single-particle spectrum is gapped out completely; from the perspective of the symmetric semimetal, this is favorable to a partial gap opening, because the reduction of density of states at the Fermi level is larger this way. Henceforth, I shall call the usual  $\text{SO}(3)$ -Néel phase  $\langle \bar{\psi} L_a \psi \rangle \neq 0$  the  $\text{SO}(3)_1$  phase; since every  $L_a$  has one zero eigenvalue, this is a semimetallic phase, but with only  $N_f/3$  gapless fermionic modes. The phase  $\langle \bar{\psi} Q_A \psi \rangle \neq 0$  I shall call  $\text{SO}(3)_2$  phase; it is an interaction-induced insulator, which I shall refer to on occasion in words as an ‘interaction-induced biadjoint insulator’ due to the way the OP  $\phi = \phi_A Q_A$  transforms under  $\text{SO}(3)$ .<sup>12</sup>

<sup>11</sup> Henceforth, manifestly representation-dependent statements—such as the nature of components of a specific generator—will be made in the defining representation.

<sup>12</sup> For  $\text{SO}(3)$ , the adjoint and fundamental representations are unitarily equivalent. Consequently, there is also a unitary map between the biadjoint representation appearing here and five-dimensional representations that arise in other contexts, where they have been referred to as “quadrupolar”/“nematic” in the study of the spin-1 Heisenberg model (cf., e.g., [35–40]), “rank-2” or simply “tensor” in the context of Luttinger semimetals (cf., e.g., [41, 42]). The present nomenclature has the advantage of making transparent the generalization from  $\text{SO}(3)$  to an arbitrary Lie group as appropriate to the context of Gross-Neveu theory with non-abelian isospin.

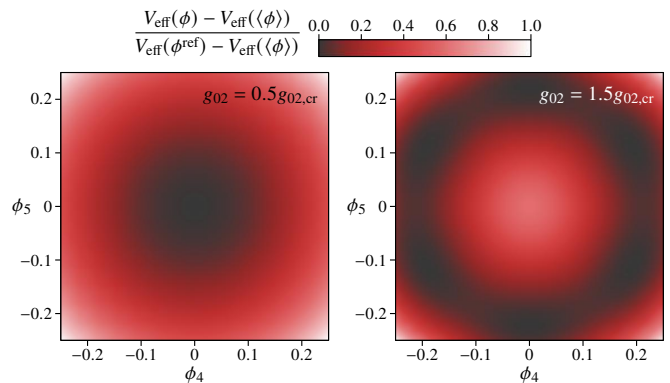


FIG. 2. Plot of the effective potential of the order parameter  $\phi = \phi_A Q_A$  for  $g_{02} < g_{02,\text{cr}}$  (left) and  $g_{02} > g_{02,\text{cr}}$  (right) in the frame  $(\phi_A) = (0, 0, 0, \phi_4, \phi_5)$  in units of  $V_{\text{eff}}(\phi^{\text{ref}}) - V_{\text{eff}}(\langle \phi \rangle)$ , where  $\phi^{\text{ref}} = (0, 0, 0, 1/4, 1/4)$  is an arbitrarily chosen reference point. The minimum is located at  $(0, \pm v)$  up to rotations in the  $(\phi_4, \phi_5)$  plane by  $n\pi/6$  ( $n \in \mathbb{Z}$ ); note that the corresponding operation on  $(Q_4, Q_5)$  sends the matrix  $Q_5$  to one that is unitarily equivalent. The critical value of the coupling  $g_{02,\text{cr}}$  can only be determined from an explicit computation, see discussion below Eq. (8). All dimensionful quantities are measured in units of the UV cutoff  $k_{\text{UV}}$ , which corresponds (roughly) to the lattice constant.

The absence or presence of a gap in the fermion spectrum is therefore one obvious way to distinguish the  $\text{SO}(3)_1$  from the  $\text{SO}(3)_2$  phase. This will manifest itself in thermodynamic measurements: e.g., in the  $\text{SO}(3)_2$  state, the electrical conductivity will show an activated behavior as a function of temperature due to the spectral gap, whilst in the  $\text{SO}(3)_1$  phase, it will follow a power law due to the leftover gapless fermionic mode.

Another way is *time-reversal symmetry*. To see this, note that the internal part of the time-reversal symmetry  $\mathcal{T}$  can be represented, in the appropriate basis, as complex conjugation  $\mathcal{K}$ :  $\mathcal{T} = \mathcal{K}$ . This happens to be the case in the *defining* representation, where the generators have components  $(L_a)_{ij} = i\epsilon_{aij}$  and are hence purely imaginary. This ensures the  $L_a$ , and consequently the Néel order parameter  $\langle \bar{\psi} L_a \psi \rangle$ , are odd under time reversal. On the other hand, the  $Q_{ab}$  in the defining representation can be checked by explicit computation to be real: the  $\text{SO}(3)_2$  order parameter  $\langle \bar{\psi} Q_{ab} \psi \rangle$  is therefore *even* under time reversal. This also has measurable consequences: for instance, in an infinitesimally weak external magnetic field (which is also odd under time reversal),  $\langle \bar{\psi} L_a \psi \rangle$  will develop an infinitesimal vev;  $\langle \bar{\psi} Q_{ab} \psi \rangle$  will not.

#### IV. BETA FUNCTIONS AND FIXED POINTS

The general algorithm developed by Gehring, Gies & Janssen [43] (= GGJ) provides a way to systematically derive the beta functions for a generic 4-Fermi theory at one-loop. Applying this formalism<sup>13</sup> to  $\mathcal{L}_{\text{GN}_3-\text{SO}(3)}$  leads to beta func-

<sup>13</sup> I am grateful to K. Ladovrechis for helpful comments on the implementation of the GGJ algorithm using computer algebra.

tions for the dimensionless 4-Fermi couplings which are given by

$$\beta_{01} = (D-2)g_{01} - \left(\frac{3}{D} - \frac{9}{2DN_f}\right)g_{01}^2 + \frac{3(12g_{00} + 36g_{10} + 12g_{11} - 15g_{12} - 5g_{02})}{2DN_f}g_{01} + \frac{3(48g_{10}g_{11} + 10g_{11}g_{12} + 15g_{12}g_{02})}{2DN_f} \quad (11)$$

$$\beta_{02} = (D-2)g_{02} - \left(\frac{3}{D} - \frac{3}{2DN_f}\right)g_{02}^2 + \frac{9(4g_{00} + 12g_{10} + g_{12} - g_{01})}{2DN_f}g_{02} + \frac{3(48g_{10}g_{12} + 3g_{11}^2 + 7g_{12}^2 + 9g_{12}g_{01})}{2DN_f} \quad (12)$$

$$\beta_{11} = (D-2)g_{11} + \left(\frac{1}{D} + \frac{27}{4DN_f}\right)g_{11}^2 + \frac{36g_{00} + 12g_{10} - 5g_{12} - 3g_{01} + 15g_{02}}{2DN_f}g_{11} + \frac{96g_{10}g_{01} + 105g_{12}^2 + 20g_{12}g_{01} + 3g_{01}^2 + 15g_{02}^2}{4DN_f} \quad (13)$$

$$\beta_{12} = (D-2)g_{12} + \left(\frac{1}{D} + \frac{1}{2DN_f}\right)g_{12}^2 + \frac{36g_{00} + 12g_{10} + 60g_{11} + 3g_{01} + 13g_{02}}{2DN_f}g_{12} + \frac{3(16g_{10}g_{02} + 2g_{11}g_{01} + 3g_{01}g_{02})}{2DN_f} \quad (14)$$

$$\beta_{00} = (D-2)g_{00} - \left(\frac{18}{D} - \frac{18}{DN_f}\right)g_{00}^2 + \frac{3(18g_{10} + 9g_{11} + 15g_{12} + 3g_{01} + 5g_{02})}{DN_f}g_{00} + \frac{36g_{10}^2 + 3g_{11}^2 + 5g_{12}^2}{DN_f} \quad (15)$$

$$\beta_{10} = (D-2)g_{10} + \left(\frac{6}{D} + \frac{6}{DN_f}\right)g_{10}^2 + \frac{18g_{00} + 3g_{11} + 5g_{12} - 3g_{01} - 5g_{02}}{DN_f}g_{10} + \frac{2(3g_{11}g_{01} + 5g_{12}g_{02})}{3DN_f} \quad (16)$$

Here,  $\beta_{r\ell} = k\partial_k g_{r\ell}$  where  $k$  is the RG scale<sup>14</sup> and  $g_{r\ell}$  are rescaled 4-Fermi couplings,  $4\nu_D l_1^{(F)D} k^{D-2} g_{r\ell} \mapsto g_{r\ell}$  in spacetime dimension  $D$ . The power  $k^{D-2}$  simply arises from the engineering (i.e., canonical scaling) dimension of 4-Fermi operators in  $D$  dimensions. The factor  $\nu_D = [2^{D+1}\pi^{D/2}\Gamma(D/2)]^{-1}$  comes from the angular part of the loop integration, and  $l_1^{(F)D}$  is a dimensionless constant that encodes the (regularized) radial part of the loop integral and drops out of universal data such as critical exponents, see [43]. Note the wavefunction renormalization  $Z_\psi = 1$  in the present approximation. Unless mentioned otherwise, I set  $D = 3$  when quoting final expressions such as fixed-point values of couplings and scaling dimensions. The determination of the quadratic beta function coefficients constitutes the major technical output of this work; I have tabulated them in electronic form for download.<sup>15</sup>

Including degeneracies and accounting for complex solutions, there are  $2^6 - 1 = 63$  interacting fixed points  $\mathcal{I}$ , in addition to the Gaussian fixed point  $\mathcal{G}$ :  $g_{r\ell,*} = 0$ . The latter corresponds to the semimetallic phase, and has no relevant directions, since the canonical dimension of 4-Fermi couplings is  $[g_{r\ell}] = 2 - D = -1$ . Some general facts about the interacting fixed points  $\mathcal{I}$  can also be proven independently of the matrix algebra appearing in the 4-Fermi Lagrangian, as was done by GGJ; these are:

(T1) The ray  $\overrightarrow{\mathcal{G}\mathcal{I}}$  is closed under RG.

(T2) All interacting fixed points  $\mathcal{I}$  have at least one relevant direction given by the fixed-point vector  $g_{r\ell,*}$  itself; the corresponding eigenvalue of the stability matrix at  $\mathcal{I}$  is  $+1$ . As such, this is an artefact of the one-loop approximation; however,  $1/\nu = -[g_{r\ell}] = D - 2$  recovers the  $D \rightarrow 2$  and  $D \rightarrow 4$  limits exactly [1, 3]. This *a priori* naive approximation hence tends to do unreasonably well in practice also at  $D = 3$ , cf., e.g., [28, 29, 32].

(T3) If this is the unique relevant direction,  $\mathcal{I}$  is called a ‘‘critical’’ fixed point. I shall notationally emphasize this by denoting such fixed points as  $\mathcal{Q}$ .

(T4) The point  $\lim_{\lambda \rightarrow \infty} \lambda \mathcal{Q} =: (+\infty)\mathcal{Q}$  represents a stable SSB phase of matter.

I shall proceed with the discussion of the pertinent fixed points as follows: First, I shall restrict the beta functions to the SU(3)-invariant subspace  $g_{r1} = g_{r2} =: g_{rV}$  and consider the fixed point that has at most one relevant direction within this subspace and remains ‘‘close’’ to the  $r = 0$  (i.e., Lorentz scalar) subspace. I shall then consider whether perturbations out of the SU(3) subspace [but preserving SO(3) symmetry] are relevant or not. For analytical tractability, I shall expand all quantities in powers of  $1/N_f$ .

## V. THE SU(3), SO(3)<sub>1</sub> AND SO(3)<sub>2</sub> FIXED POINTS AND THEIR STABILITY

The beta functions for the couplings within the SU(3) invariant subspace follow as a corollary of Eqs. (11)–(16) by setting  $g_{r1} = g_{r2} \equiv g_{rV}$ . The interacting fixed point  $\mathcal{Q}_{\text{SU}(3)}$  that describes the dynamical generation of an SU(3) breaking Lorentz scalar mass can be identified by its large- $N_f$  limit

<sup>14</sup> My sign convention for the beta function is such that a *negative* beta function means the dimensionless coupling will *grow* towards the IR. In other words,  $k \rightarrow \infty$  is the UV limit and  $k \rightarrow 0$  is the IR limit.

<sup>15</sup> See Supplemental Material (SM) for electronic version of the coefficients  $A_{r\ell}^{r_1 r_2 \ell_1 \ell_2} = \frac{1}{2} \partial^2 \beta_{r\ell} / \partial g_{r_1 \ell_1} \partial g_{r_2 \ell_2} |_{g=0}$ .

$\lim_{N_f \rightarrow \infty} g_{r,\lambda,*} = \delta_{r0}\delta_{\lambda V}$ . To second order in  $1/N_f$ , the couplings are

$$\begin{aligned} Q_{\text{SU}(3)}: g_{r,\lambda,*} = & \left(1 - \frac{1}{N_f} - \frac{8}{N_f^2}\right) \delta_{r0}\delta_{\lambda V} \\ & + \left(-\frac{3}{2N_f} + \frac{31}{4N_f^2}\right) \delta_{r1}\delta_{\lambda V} \\ & + \frac{8}{3N_f^2} \delta_{r0}\delta_{\lambda 0} + \mathcal{O}(1/N_f^3). \end{aligned} \quad (17)$$

This fixed point has a unique relevant direction *within* the SU(3)-invariant subspace. To study perturbations orthogonal to this space, consider  $\beta_{\delta g_{rV}} = \beta_{r2} - \beta_{r1}$  with  $g_{r1} = g_{rV}$ ,  $g_{r2} = g_{rV} + \delta g_{rV}$ . The beta functions for the dimensionless  $\delta g_{rV}$  have the form  $\beta_{\delta g_{rV}} = \Delta_{r,r'} \delta g_{r'V} + \mathcal{O}(\delta^2)$ . The eigenvalues of  $\Delta_{r,r'}$  at  $g_{r,\lambda} = g_{r,\lambda,*}|_{Q_{\text{SU}(3)}}$  are the scaling dimensions of SU(3) breaking perturbations that preserve SO(3). They are given by

$$\Delta_+ = 1 + \frac{32}{3N_f^2} + \mathcal{O}(1/N_f^3), \quad (18)$$

$$\Delta_- = -1 + \frac{4}{3N_f} + \frac{26}{N_f^2} + \mathcal{O}(1/N_f^3). \quad (19)$$

The eigenvalue  $\Delta_+$  corresponds to a perturbation primarily towards  $r = 1$  (= Lorentz vector) channels. On the other hand,  $\Delta_-$  corresponds to a perturbation predominantly within the Lorentz scalar subspace. For  $N_f \rightarrow \infty$ , it is *negative*: SU(3) symmetry is *not* emergent at criticality.

This result is intuitive enough to understand, once embedded within the SO(3) theory. In the strict large- $N_f$  limit, all channels decouple. As a corollary of (T2), the number of relevant directions of an interacting fixed point in this limit is then equal to the number of non-vanishing couplings. The fixed point  $Q_{\text{SU}(3)}$  is, in SO(3)-terms, the fixed point  $g_{r,\lambda,*} = \delta_{r0}(\delta_{\ell 1} + \delta_{\ell 2}) + \mathcal{O}(1/N_f)$ ; it is hence actually bicritical. In the regime of large but finite  $N_f$ , the two critical fixed points are instead

$$\begin{aligned} Q_{\text{SO}(3)_1}: g_{r,\ell,*} = & \left(1 + \frac{3}{2N_f} + \frac{3}{4N_f^2}\right) \delta_{r0}\delta_{\ell 1} \\ & - \left(\frac{1}{4N_f} + \frac{43}{48N_f^2}\right) \delta_{r1}\delta_{\ell 1} \\ & + \frac{1}{6N_f^2} \delta_{r1}\delta_{\ell 0} + \frac{1}{4N_f^2} \delta_{r1}\delta_{\ell 2} \\ & + \mathcal{O}(1/N_f^3), \end{aligned} \quad (20)$$

$$\begin{aligned} Q_{\text{SO}(3)_2}: g_{r,\ell,*} = & \left(1 + \frac{1}{2N_f} + \frac{1}{4N_f^2}\right) \delta_{r0}\delta_{\ell 2} \\ & - \left(\frac{5}{4N_f} - \frac{65}{48N_f^2}\right) \delta_{r1}\delta_{\ell 2} + \mathcal{O}(1/N_f^3). \end{aligned} \quad (21)$$

Their physics is characterized by their  $N_f \rightarrow \infty$  behavior,

$$Q_{\text{SO}(3)_\ell}: \lim_{N_f \rightarrow \infty} g_{r,\ell',*}|_{Q_{\text{SO}(3)_\ell}} = \delta_{r0}\delta_{\ell \ell'}; \quad (22)$$

they are (the finite- $N_f$  descendants of) the critical fixed points describing the interaction-induced transition to the Néel phase ( $\ell = 1$ ) and the biadjoint insulator ( $\ell = 2$ ) respectively. The phase diagram<sup>16</sup> that emerges corresponds to the one shown in the left panel of Fig. 1.

However, once  $N_f$  is decreased, the different channels begin to interact non-trivially with each other, and the eigenvalues for explicit SU(3)-breaking perturbations obtain corrections. Whether  $\Delta_-$  will be driven towards irrelevance, and whether  $\Delta_+$  will remain positive, cannot be answered *a priori*, but can only be decided by an explicit computation, the result of which is Eqs. (18)-(19). Thus, we arrive at the main result of this paper: for  $N_f \lesssim N_{f,\text{cr}}$ ,  $Q_{\text{SU}(3)}$  becomes *stable* with respect to SO(3)-invariant breaking of SU(3) symmetry. In the above approximation,  $N_{f,\text{cr}} \approx 2 + \sqrt{30} \approx 7.5$ .<sup>17</sup>

It is now worth asking, what erstwhile critical SU(3) non-invariant fixed point(s) the flow is attracted from. The two natural candidates are precisely the  $Q_{\text{SO}(3)_1}$  and  $Q_{\text{SO}(3)_2}$  discussed above. It turns out, that  $Q_{\text{SO}(3)_1}$  obtains no further relevant directions. Even at small  $N_f$ , it continues to govern the universal behavior of the Néel transition. In fact, numerically solving the beta functions shows that the fixed-point couplings  $g_{r,\ell,*}|_{Q_{\text{SO}(3)_1}}$  for  $r \neq 0$  or  $\ell \neq 1$  remain at least an order of magnitude smaller than  $g_{r,\ell,*}|_{Q_{\text{SO}(3)_1}}$ . This makes it plausible that the leading thermodynamic critical exponents derived in [32] using a battery of higher-order field theory methods but in an effectively one-channel setting for the GN<sub>3</sub>-SO(3)<sub>1</sub> transition should at most receive corrections at the 10 % level once subleading channels are included. Computations beyond 10 % accuracy, however, should ideally account for the subleading channels if they are to be reliable and internally consistent. On the other hand,  $Q_{\text{SO}(3)_2}$  develops a second relevant direction. It ceases to describe the interaction-induced transition from the symmetric semimetal to the biadjoint insulator phase. The flow towards  $(+\infty)Q_{\text{SO}(3)_2}$  is instead re-directed towards  $(+\infty)Q_{\text{SU}(3)}$ , leading to the phase diagram on the right panel of Fig. 1.

There are some technical curiosities concerning this exchange of fixed-point stability between  $Q_{\text{SO}(3)_2}$  and  $Q_{\text{SU}(3)}$ , which I wish to mention by way of closing this section:  $Q_{\text{SO}(3)_2}$  and  $Q_{\text{SU}(3)}$  live in different RG-closed subspaces of the full GN<sub>3</sub>-SO(3) theory space. As a result, they cannot collide with each other<sup>18</sup>. There is instead a bicritical fixed point  $\mathcal{B}$  not adiabatically connected to the mean-field limit, which first collides with the critical  $Q_{\text{SO}(3)_2}$  at an  $N_f = N'_{f,\text{cr}} > N_{f,\text{cr}}$  and exchanges stability with it, before proceeding to do the same with  $Q_{\text{SU}(3)}$  at  $N_f = N_{f,\text{cr}}$ . When the dust settles, (i)  $\mathcal{B}$  remains bicritical and comes to lie in the sector spanned by

<sup>16</sup> To compute the phase diagram as a function of  $g_{01}$  and  $g_{02}$ , the RG flow is initialized within the  $(g_{01}, g_{02})$  plane and integrated. Ordered phases correspond to a divergence of 4-Fermi coupling(s) within finite flow time  $t_{\text{SSB}}$ . The precise nature of the ordered phase is characterized using (T4), i.e., by comparing the (finite) ratios of 4-Fermi couplings at  $t_{\text{SSB}}$  with those obtained at the critical fixed points.

<sup>17</sup> Working to all orders in  $N_f$  by solving the fixed-point equations and determining the stability matrix eigenvalues numerically only gives modest corrections,  $N_{f,\text{cr}} \approx 6.5$ .

<sup>18</sup> I thank L. Janssen for alerting me to this.

the rays  $\overrightarrow{\mathcal{G}_{\text{SU}(3)}}$  and  $\overrightarrow{\mathcal{G}_{\text{SO}(3)_1}}$  [i.e., it separates the  $\text{SO}(3)_1$  phase from the  $\text{SU}(3)$  insulator], and (ii)  $\mathcal{Q}_{\text{SO}(3)_2}$  and  $\mathcal{Q}_{\text{SU}(3)}$  have effectively exchanged stability despite never entering each other's RG-closed subspace. There is hence also an intriguing theoretical scenario for  $N_{f,\text{cr}} < N_f < N'_{f,\text{cr}}$ , where both  $\mathcal{Q}_{\text{SO}(3)_2}$  and  $\mathcal{Q}_{\text{SU}(3)}$  are bicritical. Alas, it turns out that  $3\lfloor N_{f,\text{cr}}/3 \rfloor < N_{f,\text{cr}} < N'_{f,\text{cr}} < 3\lceil N_{f,\text{cr}}/3 \rceil$ : though interesting in its own right, this regime is not realizable for any physical flavor number  $N_f \in 3\mathbb{N}_{>0}$ . As an aside, I should point out here that the identification of the fixed points  $\mathcal{Q}_{\text{SO}(3)_\ell}$  and  $\mathcal{Q}_{\text{SU}(3)}$  relies primarily on the fact that they are connected adiabatically (in fact, differentiably as a function of  $N_f$ ) to the large- $N_f$  limit, where the associated ordered phase can be identified trivially due to the single-channel nature of the fixed points. I have checked numerically, that down to the lowest  $N_f$ 's considered here, the fixed points remain approximately single-channel, in the sense that there is a clearly dominant channel inherited from the strict large- $N_f$  limit; the remaining channels continue to be subleading in the sense that the fixed-couplings in those channels continue to be much smaller. This is shown in Fig. 3. Though an unambiguous identification of the ordering tendencies associated with these fixed points would require an analysis of the susceptibility exponents (essentially, the anomalous dimensions of all fermion bilinears with up to two  $\text{SO}(3)$ -covariant isospin indices), the relative sizes of the fixed point couplings make it reasonable to expect that the ordering preferred at mean-field level (i.e., for  $N_f = \infty$ ) continues to be valid at small  $N_f$ . Finally, the fixed point  $\mathcal{B}$  which collides with  $\mathcal{Q}_{\text{SO}(3)_2}$  at  $N_f = N'_{f,\text{cr}}$  and  $\mathcal{Q}_{\text{SU}(3)}$  at  $N_f = N_{f,\text{cr}}$  moves significantly in theory space as a function of  $N_f$ . Consequently, it is impossible to read off the leading ordering tendency by an inspection of the fixed-point couplings themselves, but would require one to perform a separate systematic study of the renormalization of the fermion bilinears themselves. This is left for future work.

## VI. THE SYMMETRY-BROKEN INSULATING PHASE: $\text{SO}(3)_2$ VS $\text{SU}(3)$

The single-particle fermion spectrum in the SSB phase is not qualitatively different in the  $\text{SU}(3)$  vis-a-vis  $\text{SO}(3)_2$  insulator phases. In both cases, the mass matrix is  $\sim Q_5 \equiv \Lambda_8$ , having no zero eigenvalue and thus leaving no gapless fermions post-SSB. However, there are sharp differences, already at the *qualitative* level, that manifest themselves in other observables, of which I shall discuss two examples.

- (i) *Number of Nambu-Goldstone bosons (NGBs)*. If the symmetry is only  $\text{SO}(3)$ , we need only consider the three generators  $L_a$ . Among them, only  $L_1$  and  $L_2$  do not commute with  $Q_5$  ( $\equiv \Lambda_8$ ). Consequently, the biadjoint insulator  $(+\infty)\mathcal{Q}_{\text{SO}(3)_2}$  has two NGBs, just like the  $\text{SO}(3)_1$  phase. On the other hand, at  $(+\infty)\mathcal{Q}_{\text{SU}(3)}$ , the emergence of  $\text{SU}(3)$  symmetry means every  $\Lambda_\alpha$  that fails to commute with  $\Lambda_8$  ( $\equiv Q_5$ ) supplies an NGB. Direct computation reveals there are hence *four* NGBs in the  $\text{SU}(3)$  insulator.

- (ii) *Divergent susceptibilities*. The large- $N_f$  universality classes are characterized by one of the  $\text{SO}(3)_\ell$  susceptibilities diverging near criticality, while the other one remains finite. In the  $\text{SU}(3)$  transition, however, both the  $\text{SO}(3)_1$  and  $\text{SO}(3)_2$  order parameters transform as components of an adjoint vector under  $\text{SU}(3)$ . Consequently, in addition to a divergent  $\text{SO}(3)_2$  susceptibility, one will now have a divergent  $\text{SO}(3)_1$  susceptibility at the transition to the interaction-induced insulator with spontaneously broken isospin symmetry.

Both examples constitute robust signatures that may be expected to survive beyond the present approximation. Furthermore, (ii) is practically interesting: a completely gapped fermion spectrum in the SSB phase accompanied by a divergent  $\text{SO}(3)_1$  susceptibility is a “smoking-gun” signature one can search for in experiments to verify whether  $\text{SU}(3)$  isospin symmetry emerges or not at the transition to the insulating SSB phase.

## VII. OUTLOOK: SOME APPLICATIONS

A recent Letter [44] presented Quantum Monte Carlo simulations of an  $N_f = 12$   $\text{GN}_3$ - $\text{SO}(3)_1$  transition using a  $t$ - $V$  model with Hamiltonian of the form

$$H = H_t + H_V \quad (23)$$

$$H_t = t \sum_{\langle ij \rangle} c_{i\sigma}^\dagger c_{j\sigma} + \text{H.c.} \quad (24)$$

$$H_V = V \sum_i \left( c_{i\sigma}^\dagger L_a^{\sigma\sigma'} c_{i\sigma'} \right)^2 \quad (25)$$

where  $c_{i\sigma}^\dagger$  ( $c_{i\sigma}$ ) creates (annihilates) a fermion with  $\text{SO}(3)$  quantum number  $\sigma$  at site  $i$  of a honeycomb lattice, and  $\langle ij \rangle$  denotes nearest-neighbor bonds. (The cited reference also had a bilayer index, which I shall neglect here.) Interestingly, a further quantum phase transition from the Néel semimetal phase to an interaction-induced SSB insulator phase was found. The latter phase was diagnosed to have vanishing Néel order parameter and a spontaneously broken  $U(1)$  symmetry. Assuming the absence of a narrow coexistence phase or a weak first-order transition, this would be a classically forbidden order-to-order quantum phase transition, and has been suggested to be a candidate for a so-called deconfined quantum critical point. The findings I have presented raise the intriguing possibility of tuning an  $\text{SO}(3)$  Dirac system through a further interaction-induced Néel-to-SSB insulator transition by including the perturbation

$$H_{V'} = 4V' \sum_i \left( c_{i\sigma}^\dagger Q_A^{\sigma\sigma'} c_{i\sigma'} \right)^2, \quad (26)$$

which has the same symmetries as  $H_V$ , and tuning close to the  $\text{SU}(3)$ -invariant point. This continuous transition would be governed by a conventional bicritical endpoint. Critical exponents measured at this transition would be an interesting point of comparison: if they are indeed very different from those

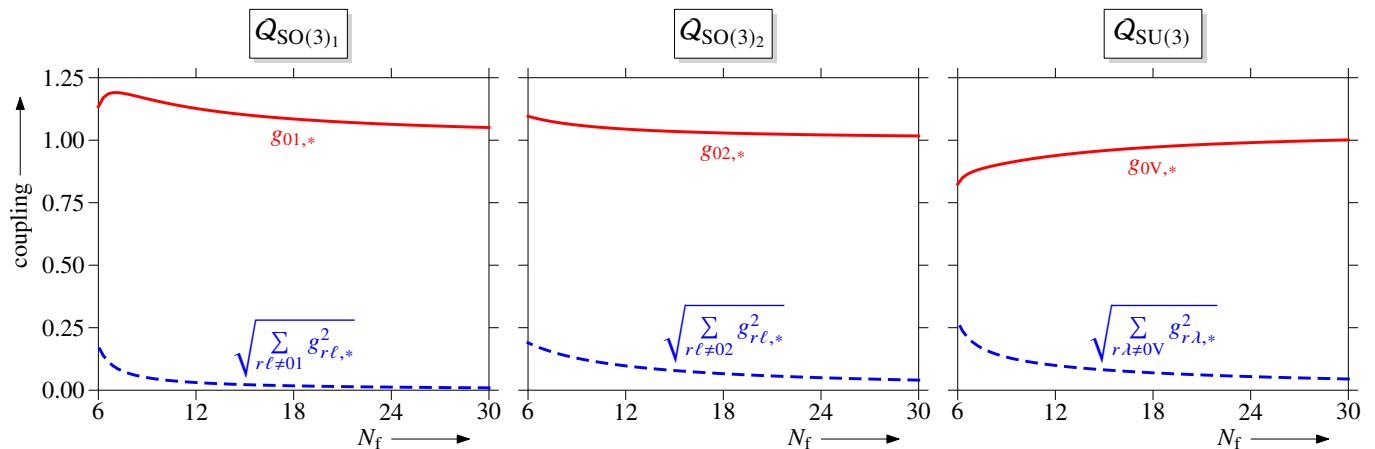


FIG. 3. Values of 4-Fermi couplings at fixed points  $Q_{\text{SO}(3)_\ell}$  ( $\ell = 1, 2$ ) and  $Q_{\text{SU}(3)}$ , showing the nearly single-channel nature of these fixed points persists down to small  $N_f$ .

one could measure at the putative deconfined quantum critical point of [44], then this would point towards a genuinely different underlying mechanism. On the other hand, if the two sets of exponents are close to each other, one may be motivated to look for whether other aspects of the observed phenomenology may in fact be describable by a conventional mechanism.

Furthermore, using  $H_t + H_{V'}$  as a starting point (i.e.,  $V/t \ll V'/t$ ), one should be able to also simulate a pure  $\text{GN}_3\text{-SO}(3)_2$  transition (note that  $N_f = 12$  is well above the critical flavor number below which  $\text{SU}(3)$  becomes emergent at the insulating transition). Furthermore,  $N_f = 12$  is large enough for the  $1/N_f$  to provide reliable theoretical benchmarks already at low orders. Interestingly, for the  $\text{GN}_3\text{-SO}(3)_1$  transition, (some of) the critical exponents determined numerically in [44] showed significant deviations from the theoretical prediction. It would be interesting to see whether a similar discrepancy presents itself also for the  $\text{GN}_3\text{-SO}(3)_2$  transition.

Beyond numerical experiments, there are also candidate materials that have been suggested to realize  $\text{SO}(3)$  quantum spin-orbital liquid (= spinon semimetal) ground states [25–27]. Critical exponents governing thermodynamic observables of quantum phase transitions from a spin-orbital liquid phase to magnetically ordered phases provide insight into the nature of the otherwise experimentally elusive spinons, such as their isospin symmetry. The present findings suggest one could do so in at least one “orthogonal” direction—viz., the biadjoint insulator—in addition to the Néel phase. If the two interaction-induced transitions can be tuned independently of each other, there would be twice as many independent quantities [i.e.,  $\nu_{\text{SO}(3)_1}, \gamma_{\text{SO}(3)_1}, \nu_{\text{SO}(3)_2}, \gamma_{\text{SO}(3)_2}$ ] which may be measured in principle. Such combined measurements would allow one to constrain the admissible isospin content of spinons in putative quantum spin-orbital liquids more sharply than when considering the Néel transition in isolation. This is a tantalising prospect and suggests a more concerted attack in future investigations from several angles:

1. On the theoretical side, it would be worthwhile to subject the critical exponents of the  $\text{GN}_3\text{-SO}(3)_2$  and  $\text{GN}_3\text{-SU}(3)$  universality class to a battery of more sophisticated techniques, along the lines of what was done for  $\text{GN}_3\text{-SU}(2)$  in [29, 30] or  $\text{GN}_3\text{-SO}(3)_1$  in [32].
2. On the phenomenological side, one would like to identify what microscopic interaction gives birth to the  $g_{02}$  4-Fermi coupling. (Note that here, one needs to identify an interaction between spin-orbital moments, unlike the setting of [44] where one can start with itinerant fermions and Eq. (26) yields the desired construction.) In spin-1 magnets, spin-nematic phases are stabilized by a biquadratic generalization of the Heisenberg interaction [36, 38–40]. For the spin-orbital model of [25], the explicit form of the corresponding generalization, though just as symmetry-allowed, is less clear, at least to me.
3. On the ab initio side, once the pertinent microscopic spin-orbital interaction has been identified, it would be interesting to compute what is the microscopic value of this new interaction in candidate  $\text{SO}(3)$  spin-orbital liquids such as  $\text{Ba}_2\text{YMoO}_6$  and twisted-bilayer  $\alpha\text{-RuCl}_3$ .

## ACKNOWLEDGMENTS

I thank K. Ladovrechis, T. Meng, G. P. de Brito, M. M. Scherer, L. Janssen and A. Eichhorn for discussions and collaboration on related projects. I am moreover indebted to the last three of the aforementioned for carefully reading and providing helpful comments on earlier versions of this manuscript. Further enlightening discussions with A. A. Christensen and G. J. Jensen are gratefully acknowledged. This work has been supported by a research grant (29405) from VILLUM FONDEN and partially by the Deutsche Forschungsgemeinschaft (DFG) through the Walter Benjamin program (RA3854/1-1, Project id No. 518075237).



- [1] J. Cardy, *Scaling and renormalization in statistical physics* (Cambridge University Press, 1996).
- [2] S. Sachdev, *Quantum Phase Transitions*, 2nd ed. (Cambridge University Press, 2011).
- [3] I. Herbut, *A Modern Approach to Critical Phenomena* (Cambridge University Press, 2007).
- [4] S.-S. Lee, Low-energy effective theory of Fermi surface coupled with U(1) gauge field in 2 + 1 dimensions, *Phys. Rev. B* **80**, 165102 (2009).
- [5] M. A. Metlitski and S. Sachdev, Quantum phase transitions of metals in two spatial dimensions. I. Ising-nematic order, *Phys. Rev. B* **82**, 075127 (2010).
- [6] M. A. Metlitski and S. Sachdev, Quantum phase transitions of metals in two spatial dimensions. II. Spin density wave order, *Phys. Rev. B* **82**, 075128 (2010).
- [7] S. Sur and S.-S. Lee, Chiral non-Fermi liquids, *Phys. Rev. B* **90**, 045121 (2014).
- [8] S. Sur and S.-S. Lee, Quasilocal strange metal, *Phys. Rev. B* **91**, 125136 (2015).
- [9] A. Schlieff, P. Lunts, and S.-S. Lee, Exact Critical Exponents for the Antiferromagnetic Quantum Critical Metal in Two Dimensions, *Phys. Rev. X* **7**, 021010 (2017).
- [10] F. Borges, A. Borissov, A. Singh, A. Schlieff, and S.-S. Lee, Field-theoretic functional renormalization group formalism for non-Fermi liquids and its application to the antiferromagnetic quantum critical metal in two dimensions, *Ann. Phys. (N. Y.)* **450**, 169221 (2023).
- [11] I. F. Herbut, Interactions and Phase Transitions on Graphene's Honeycomb Lattice, *Phys. Rev. Lett.* **97**, 146401 (2006).
- [12] I. F. Herbut, V. Juričić, and B. Roy, Theory of interacting electrons on the honeycomb lattice, *Phys. Rev. B* **79**, 085116 (2009).
- [13] I. F. Herbut, V. Juričić, and O. Vafek, Relativistic Mott criticality in graphene, *Phys. Rev. B* **80**, 075432 (2009).
- [14] S. Pujari, T. C. Lang, G. Murthy, and R. K. Kaul, Interaction-Induced Dirac Fermions from Quadratic Band Touching in Bilayer Graphene, *Phys. Rev. Lett.* **117**, 086404 (2016).
- [15] S. Ray, M. Vojta, and L. Janssen, Quantum critical behavior of two-dimensional Fermi systems with quadratic band touching, *Phys. Rev. B* **98**, 245128 (2018).
- [16] J. N. Leaw, H.-K. Tang, P. Sengupta, F. F. Assaad, I. F. Herbut, and S. Adam, Electronic ground state in bilayer graphene with realistic Coulomb interactions, *Phys. Rev. B* **100**, 125116 (2019).
- [17] S. Ray and L. Janssen, Gross-Neveu-Heisenberg criticality from competing nematic and antiferromagnetic orders in bilayer graphene, *Phys. Rev. B* **104**, 045101 (2021).
- [18] N. Lopes, M. A. Continentino, and D. G. Barci, Excitonic insulators and Gross-Neveu models, *Phys. Rev. B* **105**, 165125 (2022).
- [19] M. Vojta, Y. Zhang, and S. Sachdev, Quantum Phase Transitions in  $d$ -Wave Superconductors, *Phys. Rev. Lett.* **85**, 4940 (2000).
- [20] R. Boyack, H. Yerzhakov, and J. Maciejko, Quantum phase transitions in Dirac fermion systems, *Eur. Phys. J. Spec. Top.* **230**, 979 (2021).
- [21] J. Braun, H. Gies, and D. D. Scherer, Asymptotic safety: A simple example, *Phys. Rev. D* **83**, 085012 (2011).
- [22] M. Reuter and F. Saueressig, *Quantum Gravity and the Functional Renormalization Group: The Road towards Asymptotic Safety* (Cambridge University Press, 2019).
- [23] A. Bonanno, A. Eichhorn, H. Gies, J. M. Pawłowski, R. Percacci, M. Reuter, F. Saueressig, and G. P. Vacca, Critical reflections on asymptotically safe gravity, *Front. in Phys.* **8**, 269 (2020).
- [24] A. Eichhorn, Status update: Asymptotically safe gravity-matter systems, *Nuovo Cim.* **C 45**, 29 (2022).
- [25] U. F. P. Seifert, X.-Y. Dong, S. Chulliparambil, M. Vojta, H.-H. Tu, and L. Janssen, Fractionalized Fermionic Quantum Criticality in Spin-Orbital Mott Insulators, *Phys. Rev. Lett.* **125**, 257202 (2020).
- [26] W. M. H. Natori, E. C. Andrade, E. Miranda, and R. G. Pereira, Chiral Spin-Orbital Liquids with Nodal Lines, *Phys. Rev. Lett.* **117**, 017204 (2016).
- [27] J. Romhányi, L. Balents, and G. Jackeli, Spin-Orbit Dimers and Noncollinear Phases in  $d^1$  Cubic Double Perovskites, *Phys. Rev. Lett.* **118**, 217202 (2017).
- [28] L. Janssen and I. F. Herbut, Antiferromagnetic critical point on graphene's honeycomb lattice: A functional renormalization group approach, *Phys. Rev. B* **89**, 205403 (2014).
- [29] B. Knorr, Critical chiral Heisenberg model with the functional renormalization group, *Phys. Rev. B* **97**, 075129 (2018).
- [30] N. Zerf, L. N. Mihaila, P. Marquard, I. F. Herbut, and M. M. Scherer, Four-loop critical exponents for the Gross-Neveu-Yukawa models, *Phys. Rev. D* **96**, 096010 (2017).
- [31] J. A. Gracey, Large  $N$  critical exponents for the chiral Heisenberg Gross-Neveu universality class, *Phys. Rev. D* **97**, 105009 (2018).
- [32] S. Ray, B. Ihrig, D. Kruti, J. A. Gracey, M. M. Scherer, and L. Janssen, Fractionalized quantum criticality in spin-orbital liquids from field theory beyond the leading order, *Phys. Rev. B* **103**, 155160 (2021).
- [33] K. Ladovrechis, S. Ray, T. Meng, and L. Janssen, Gross-Neveu-Heisenberg criticality from  $2 + \epsilon$  expansion, *Phys. Rev. B* **107**, 035151 (2023).
- [34] M. Moshinsky, J. Patera, R. Sharp, and P. Winternitz, Everything you always wanted to know about  $SU(3) \supset O(3)$ , *Ann. Phys. (N. Y.)* **95**, 139 (1975).
- [35] F. Mila and F.-C. Zhang, On the origin of biquadratic exchange in spin 1 chains, *Eur. Phys. J B* **16**, 7 (2000).
- [36] K. Harada and N. Kawashima, Quadrupolar order in isotropic Heisenberg models with biquadratic interaction, *Phys. Rev. B* **65**, 052403 (2002).
- [37] S. Bhattacharjee, V. B. Shenoy, and T. Senthil, Possible ferro-spin nematic order in  $\text{NiGa}_2\text{S}_4$ , *Phys. Rev. B* **74**, 092406 (2006).
- [38] A. Läuchli, F. Mila, and K. Penc, Quadrupolar phases of the  $S = 1$  bilinear-biquadratic Heisenberg model on the triangular lattice, *Phys. Rev. Lett.* **97**, 087205 (2006).
- [39] H. Tsunetsugu and M. Arikawa, Spin nematic phase in  $S = 1$  triangular antiferromagnets, *J Phys. Soc. Jpn.* **75**, 083701 (2006).
- [40] A. Völl and S. Wessel, Spin dynamics of the bilinear-biquadratic  $S = 1$  Heisenberg model on the triangular lattice: A quantum Monte Carlo study, *Phys. Rev. B* **91**, 165128 (2015).
- [41] I. Boettcher and I. F. Herbut, Unconventional Superconductivity in Luttinger Semimetals: Theory of Complex Tensor Order and the Emergence of the Uniaxial Nematic State, *Phys. Rev. Lett.* **120**, 057002 (2018).
- [42] L. Janssen and I. F. Herbut, Nematic quantum criticality in three-dimensional Fermi system with quadratic band touching, *Phys. Rev. B* **92**, 045117 (2015).
- [43] F. Gehring, H. Gies, and L. Janssen, Fixed-point structure of low-dimensional relativistic fermion field theories: Universality classes and emergent symmetry, *Phys. Rev. D* **92**, 085046 (2015).
- [44] Z. H. Liu, M. Vojta, F. F. Assaad, and L. Janssen, Metallic and Deconfined Quantum Criticality in Dirac Systems, *Phys. Rev. Lett.* **128**, 087201 (2022).